

ELECTRONIC AND OPTICAL PROPERTIES MODULATION OF LaCuOSe BY STRAIN

M. KASHIF^{a,*}, A. SHAHZAD^a, N. NASIR^b, K. KAMRAN^c, T. MUNIR^a,
M. S. SHIFA^d, M. YASEEN^b, A. HUSSAIN^a, N. ANJUM^a, S. GHANI^e

^a Physics Department, Govt College University Faisalabad (GCUF),
Allama Iqbal Road, Faisalabad 38000, Pakistan

^b Department of Applied Sciences, Faculty of Science, National Textile
University, Sheikhupur Road, Faisalabad, Pakistan

^c Department of Physics, University of Agriculture, Faisalabad, Pakistan

^d Institute of Physics, The Islamia University of Bahawalpur, Bahawalpur,
Pakistan

^e Department of Physics, University of Engineering and Technology,
Lahore, Pakistan

Due to promising properties of wide band gap semiconductor, they are used in optoelectronic applications. LaCuOSe is a wide bandgap semiconductor with band gap of 2.8 eV and shows extraordinary optoelectronic properties, high hole mobility and stable excitons. To study the effect of strain on the electronic and optical properties of LaCuOSe these properties were calculated under axial strain by using full potential linearized augmented plane-wave (FP-LAPW) method based on density functional theory (DFT) within GGA functional. The computed structural lattice parameters are in good agreement with the previous simulated and experimental results. The energy band structures, density of states, and optical properties are calculated and analyzed with and without strain. The results show that, by increasing the tensile strain, the band gap of LaCuOSe increases as compared to unstrained LaCuOSe and decreases with increasing the compressive strain. The biaxial strain affects the absorption of LaCuOSe and shows blue and red shift. This study shows that band gap and optical properties can tune with biaxial strain.

(Received September 8, 2020; Accepted January 21, 2021)

Keywords: First principles calculation, Strained study, Electronic properties and optical properties

1. Introduction

Layered oxychalcogenides such as LaCuOCh (Ch=S, Se, Te) have attracted much attention due to their transparent p-type semiconducting behavior [1-3]. LaCuOSe shows p-type semiconducting behavior with wide bandgap of 2.8 eV. The crystal structure of LaCuOSe consists of (La₂O₂)²⁺ oxide layers and Cu₂Se₂²⁻ layers which are alternately stacked along the c axis as shown

*Corresponding author: mkashif@gcuf.edu.pk

in Fig. 1. $\text{Cu}_2\text{Se}_2^{2-}$ layers consist of edge sharing CuCh_4 tetrahedra. LaCuOSe shows extraordinary optoelectronic properties, high hole mobility and stable excitons.

Due to these properties LaCuOSe is attractive material for optoelectronic application. Various studies have been taken to investigate the optical and electronic properties of the LaCuOSe by many researchers [4-8]. Electronic properties of LaCuOSe can be tune with doping such as Mg doping increase, the high-density hole doping up to $1.7 \times 10^{21} \text{ cm}^{-3}$ and are suitable for anode material [9]. However, the previous studies did not include the effect of strain on the LaCuOSe properties. In this studies the effect of the biaxial strain on the LaCuOSe properties are carried out.

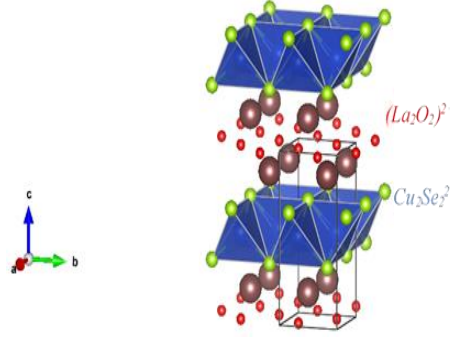


Fig. 1. Crystal structure of LaCuOSe, with $(\text{La}_2\text{O}_2)^{2+}$ oxide layers and $\text{Cu}_2\text{Se}_2^{2-}$ layers.

2. Methodology

The electronic, and optical properties of strained LaCuOSe were determined using the full-potential linearized augmented plane waves (FLAPW) method implemented in WIEN2K [10-12].

In present work, Muffin-tin radii (RMT) values for La, Cu, O, Se (2.28, 2.31, 2.20, 1.96) were used. We have optimized the $\text{RMT} \times K_{\text{max}}$ value and it is equal to 7 (kept constant) for all calculation in interstitial area and Fourier expansion of charge density, $G_{\text{max}} = 14$ is kept constant. 1000 k-points were employed for the Brillouin zone integrations to calculate the electronic and optical properties. The total energy convergence is within 0.0001 Ry. Biaxial strain is calculated

with this relation $\delta a = \frac{a - a_o}{a_o}$ where a_o is optimized lattice parameter without strain and a is

lattice parameter with strain.

3. Results and discussion

3.1. Structural properties

LaCuOSe having $P4/nmm$ (No. 129) space group are composed of layers $(\text{La}_2\text{O}_2)^{2+}$ and layers $(\text{Cu}_2\text{Se}_2)^{2-}$ which are stacked along the c axis in the tetragonal unit cell.

Structural optimizations of LaCuOSe were performed using GGA-PBE with different variations in the volume to find the equilibrium lattice constant with minimum energy. The volume vs energy curve was fitted to Murnaghan equation of state to calculate the equilibrium cell

volume. The calculated a and c lattice parameters for LaCuOSe are 4.01 Å and 8.73 Å respectively. The optimized lattice constants of LaCuOSe structure are summarized in Table 1. The current calculated lattice constants of LaCuOSe are in good agreement with previous results.

Table 1. Calculated lattice parameters of LaCuOSe.

Materials and structural Properties	Experimental results	Present results
a (Å)	4.07 ^a	4.01
c (Å)	8.80 ^a	8.73

^a Ref. [13]

3.2. Electronic properties

3.2.1. Energy bands and DOSs

The calculated band structure for LaCuOSe under biaxial strain compressive and tensile is shown in Fig. 2. The valence band maximum (VBM) and conduction band minimum (CBM) both occur at the gamma point, resulting in a fundamental band gap of 1.67 eV, which is less than the experimentally measured gap of 2.80 eV due to well know underestimation of DFT. From the figure it can be observe biaxial strain (compressive and tensile) have different influence on the energy band gap of LaCuOSe. Band Structure of LaCuOSe shows that it has direct band gap due to the VBM and CBM at the gamma point and it is observed that under biaxial strain it remain direct bap semiconductor. It can be observed that the band gap increases under tensile strain, but decreases under compressive strain which shows the band gap modulation under biaxial strain. Table-2 shows the variation of band gap values with the biaxial strains.

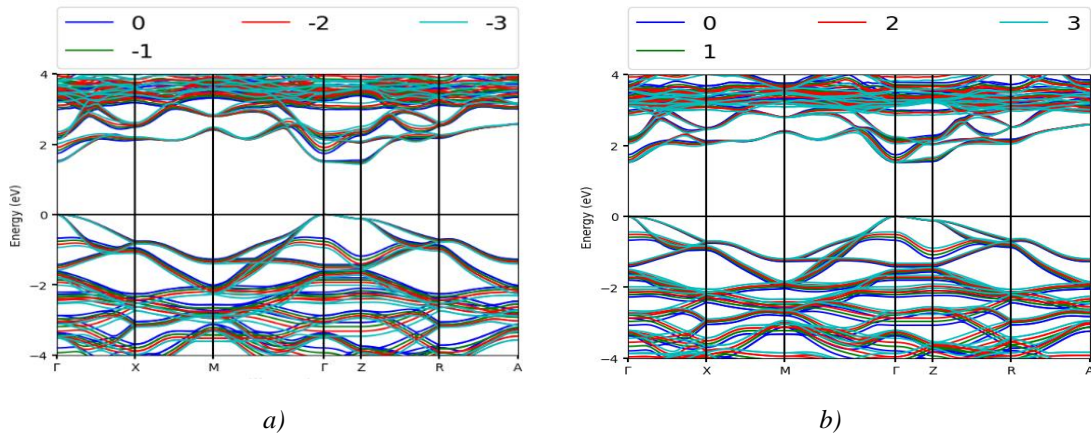


Fig. 2. Calculated band structure of LaCuOSe (a) Tensile strains of +1%, +2% and +3% (b) compressive strains of -1%, -2% and -3%.

Table 2. Calculated band gaps without and with Strain concentration ($\pm 1\%$, $\pm 2\%$ and $\pm 3\%$).

without strain (eV)	+1% (Strained) (eV)	+2% (Strained) (eV)	+3% (Strained) (eV)	-1% (Strained) (eV)	-2% (Strained) (eV)	-3% (Strained) (eV)
1.67	1.68	1.69	1.69	1.64	1.62	1.61

Fig. 3 shows the Partial density of states (PDOS) of the LaCuOSe structure. It is observed that the top of the valance band from the energy range 0 to -3eV is composed of Cu-3d and Se-p states and this region represents the anti-bonding character. This shows the strong hybridization of Cu-d and Se-p states. The region between the energy -3eV to -6 eV O-2p state is dominated with small contribution from the Se-s and Cu-3d states. The conduction band minimum is mainly composed of Cu-4s and Se-p states. Fig-4 represent the total density of states of LaCuOSe under different states. From total DOS plots, we can see that the lower edge of VBM and CBM moves towards lower energy range by increasing tensile strain and in case compressive strain moves towards higher energy. With increasing the in-plane biaxial tensile strain, the energy gap between VBM and CBM also increases and decreases with compressive strain.

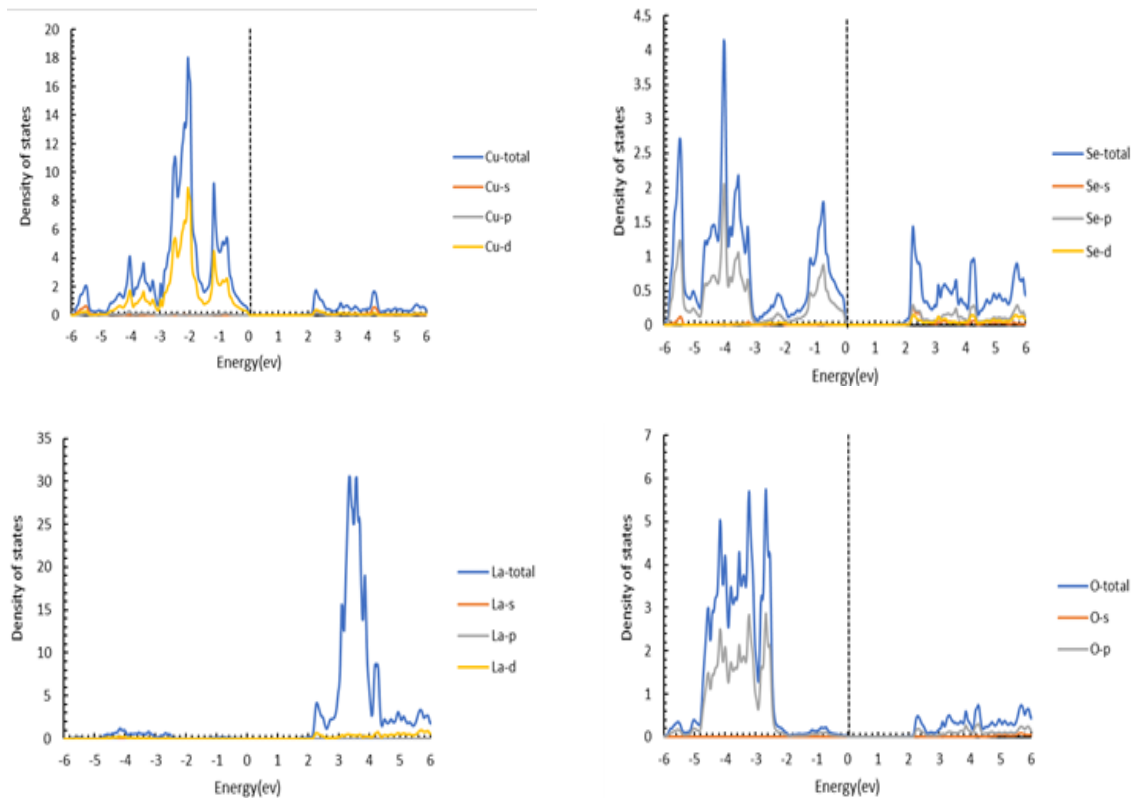


Fig. 3. Calculated partial density of states of LaCuOSe.

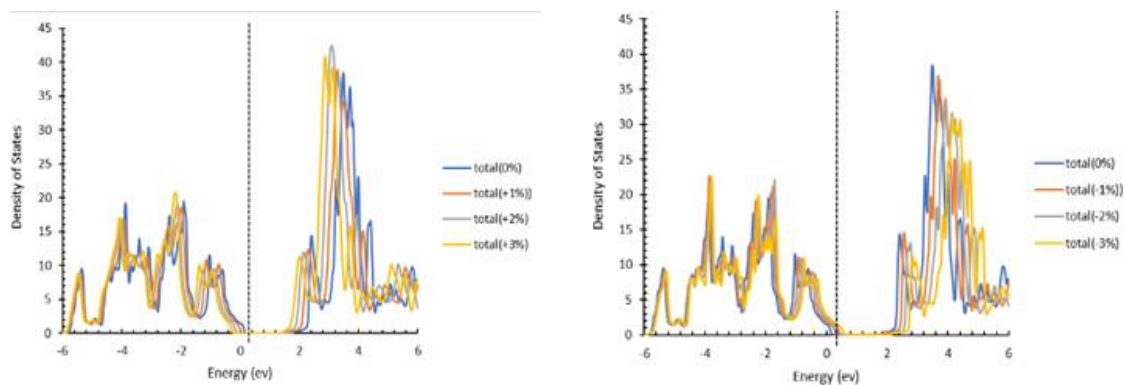


Fig. 4. Calculated total density of states of LaCuOSe under different strains.

3.3. Optical properties

The real part of the calculated dielectric function for unstrained and strained LaCuOSe is shown in Fig. 5. For the unstrained LaCuOSe the static value ($\omega=0$) of dielectric constant = 7.51. It is observed with compressive strain it is increases and decrease with tensile strain. Table 3 shows the dielectric constant values with different strains.

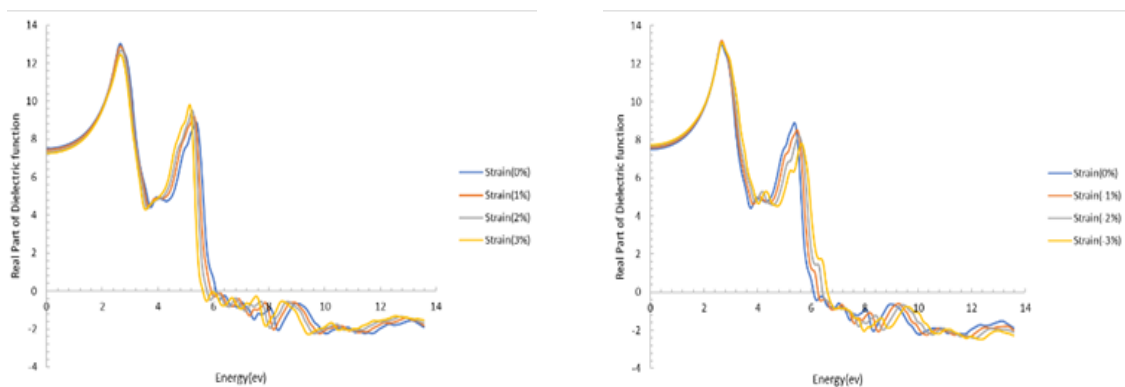


Fig. 5. Real parts of dielectric function of LaCuOSe.

Table 3. Calculated dielectric constant without and with Strain concentration ($\pm 1\%$, $\pm 2\%$ and $\pm 3\%$).

without strain	+1% (Strained)	+2% (Strained)	+3% (Strained)	-1% (Strained)	-2% (Strained)	-3% (Strained)
7.51	7.43	7.33	7.27	7.60	7.67	7.74

The absorption spectra of LaCuOSe under different strains are shown in the Fig. 6. It is observed that strong absorption peaks exist at energy range of 3 and 6.3 eV which shows that threshold of absorption spectrum lie in the visible region, but the maximum value of absorption takes place in the ultra-violet region. With the strains the absorption peaks show blue and red

shift due to compressive and tensile strain respectively but the shape of the absorption spectra remains the same. From these results we can see absorption property of the LaCuOSe can be modulate with strain.

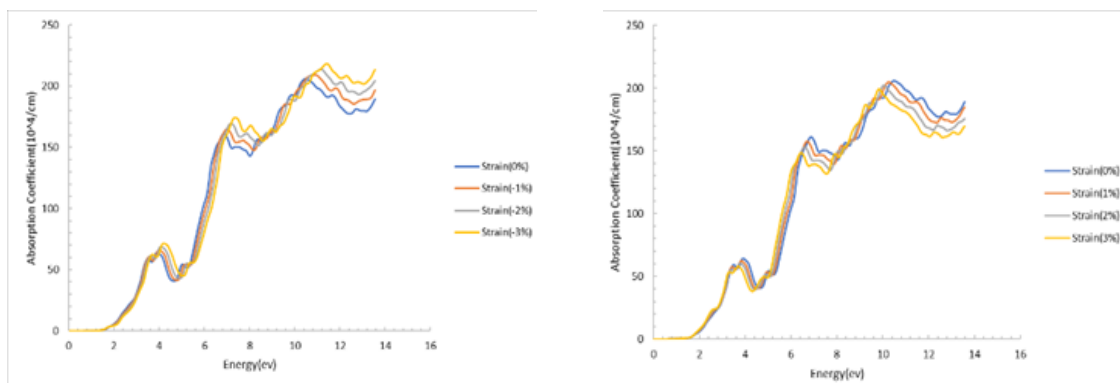


Fig. 6. Absorption of 1%,2% and 3% strain effect of LaCuOSe.

4. Conclusion

In this research work the electronic and optical properties of *LaCuOSe* under biaxial strain ($\pm 1\%$, $\pm 2\%$ and $\pm 3\%$) has been studied by using the first-principles method based on density functional theory. Band gap of LaCuOSe changes with tensile and compressive strain. The biaxial strain effects the absorption of LaCuOSe and shows blue and red shift. This study shows that band gap and optical properties can tune with biaxial strain.

Acknowledgements

The computational facilities for this work were provided by Department of Physics, Govt College University Faisalabad and Department of Physics, University OF Agriculture Faisalabad.

References

- [1] S. D. Luu, P. Vaqueiro, *Semiconductor Science and Technology* **29**, 064002 (2014).
- [2] B. A. Popovkin, A. M. Kusainova, V. A. Dolgikh, G. Akselrud, *Russian Journal of Inorganic Chemistry* **43**, 1471 (1998).
- [3] W. J. Zhu, Y. Z. Huang, C. Dong, Z. X. Zhao, *Materials Research Bulletin* **29**, 143 (1994).
- [4] H. Kamioka, H. Hiramatsu, H. Ohta, M. Hirano, K. Ueda, T. Kamiya, H. Hosono, *Applied Physics Letters* **86**, 879 (2004).
- [5] S. Inoue, K. Ueda, H. Hosono, N. Hamada, *Physical Review B* **64**, 245211 (2001).
- [6] H. Hiramatsu, K. Ueda, H. Ohta, M. Orita, M. Hirano, H. Hosono, *Thin Solid Films* **411**, 125 (2002).
- [7] H. Hiramatsu, K. Ueda, H. Ohta, M. Orita, M. Hirano, H. Hosono, *Applied Physics Letters*

- 81**, 598 (2002).
- [8] H. Sato, H. Negishi, A. Wada, A. Ino, S. Negishi, C. Hirai, H. Namatame, M. Taniguchi, K. Takase, Y. Takahashi, T. Shimizu, Y. Takano, K. Sekizawa, *Physical Review B* **68**, 035112 (2003).
- [9] H. Hiramatsu, K. Ueda, H. Ohta, M. Hirano, M. Kikuchi, H. Yanagi, T. Kamiya, H. Hosono, *Applied Physics Letters* **91**, 012104 (2007).
- [10] T. Munir, M. Kashif, W. Hussain, A. Shahzad, M. Imran, A. Ahmed, N. Amin, N. Ahmed, A. Hussain, M. Noreen, *Journal of Ovonic Research* **14**, 5(2018).
- [11] N. Nasir and M. Kashif and T. Munir and A. Shahzad, M. Noreen, K. Kamran, A. Hussain, A. Ahmed, *Digest Journal of Nanomaterials and Biostructures* **14**, 4(2019).
- [12] M. Yaseen, H Ambreen, U Shoukat, Mk Butt, S Noreen, Shafiq urRehman, J Iqbal, Shamsa Bibi, A. Murtaza, And S.M. Ramay, *Journal of Ovonic Research*, **15**, 401(2019).
- [13] Y. Ohki, S. Komatsuzaki, Y. Takahashi, K. Takase, Y. Takano, and K. Sekizawa, In *AIP Conference Proceedings* **850**(1), 1309 (2006).